Proceedings World Geothermal Congress 2026
Calgary, Canada, June 8 – 11, 2026

Experimental Evaluation on Liquid Nitrogen Cooling and Cryogenic Fracturing in High-Temperature Formations

Bowen Yao[1]*, Yu-Shu Wu[2], Ruitian Yu[3], Ding Yan[1], Hanzhong Si[1] and Hua Hua[4]
China University of Petroleum - Beijing[1]*, Colorado School of Mines[2], Tsinghua University[3], Institute of Electrical Engineering, Chinese Academy of Sciences
bowenyao@cup.edu.cn

Keywords: Geothermal, liquid nitrogen fracturing, cryogenic fracturing, productivity enhancement.

ABSTRACT

Liquid nitrogen (LN_2) cryogenic fracturing is a promising waterless stimulation technology for high-temperature hot dry rock (HDR) in Enhanced Geothermal Systems (EGS), owing to its strong "thermal shock" effect. However, systematic insights into how fracture geometry and injection parameters influence near-wellbore thermal recovery and stimulation performance remain limited. This study establishes a true-triaxial cryogenic injection system to examine LN_2 cooling and fracturing behaviors using 200 °C concrete blocks as HDR analogs. LN_2 circulation and injection tests were conducted on intact samples, vertical-fractured samples, horizontal/inclined-horizontal fractured samples, and interbedded "sandwich" structures. Internal temperature evolution was tracked with embedded thermocouples, while wellbore warm-up time (across multiple thresholds) and pressure-decay curves were compared to evaluate cooling efficiency and permeability evolution under varying injection pressures, fracture orientations, and fracture conductivities. Results show that LN_2 rapidly reduces near-wellbore temperature and forms an asymmetric, anisotropic cooling zone. Warm-up time effectively reflects both cooling extent and "cold-storage" capacity. Under similar conditions, horizontal and inclined-horizontal fractures generate larger cooled regions and longer warm-up times than vertical fractures. An optimal range exists between injection pressure and fracture conductivity: low conductivity restricts effective fracture initiation, whereas overly high conductivity causes rapid LN_2 leakoff and weakens cooling. LN_2 circulation and injection also alter fracture properties, with some samples showing accelerated post-treatment pressure decay, indicating enhanced fracture connectivity. These findings provide experimental support for optimizing LN_2-assisted EGS wellbore cooling and near-wellbore stimulation designs and for calibrating coupled thermo-hydro-mechanical simulation models.

1 INTRODUCTION

As a clean and sustainable renewable energy source, geothermal energy has attracted global attention for its ability to provide stable base-load power (BP, 2018; Global CCS Institute, 2013; Matek, 2016). Unlike solar and wind energy, which are limited by weather conditions, geothermal energy offers the advantage of round-the-clock operation. However, the vast majority of global geothermal resources are stored in hot dry rock (HDR) formations, which are typically deeply buried, high-temperature, and characterized by dense rock matrices with extremely low permeability (Brown, 2000). To efficiently extract heat from these formations, the development of Enhanced Geothermal Systems (EGS) is essential. The core technology of EGS lies in constructing artificial fracture networks in tight rock masses through hydraulic stimulation, thereby significantly improving fluid injectivity and heat exchange efficiency (Pruess, 2006; Xu et al., 2015).

For EGS reservoir stimulation, experimental research has long been a crucial means to explore fracture initiation and propagation mechanisms. Traditional hydraulic fracturing experiments have confirmed the effectiveness of water-based fluids in fracture creation but have also revealed their limitations under specific geological conditions (Harto et al., 2013). For instance, water injection in clay-rich formations can cause clay swelling and particle migration, leading to pore channel blockage and reservoir damage. Additionally, the substantial water consumption in arid regions constitutes a non-negligible constraint (Xu et al., 2008). To address these issues, numerous studies have been conducted on fracturing with non-aqueous fluids such as supercritical CO_2 and gaseous N_2. These experiments primarily focus on evaluating the effects of different fluid media on rock breakdown pressure and fracture complexity, aiming to identify more environmentally friendly and efficient stimulation fluids (Fouillac et al., 2004; Global CCS Institute, 2016).

Beyond experimental research, numerical simulation is widely used to predict fracturing behavior and thermo-hydro-mechanical (THM) coupling processes under complex geological conditions (Buscheck et al., 2014).

However, existing simulation studies often rely on simplified physical model assumptions and lack experimental data validation for specific operating conditions, particularly under extreme temperature difference scenarios (Buscheck et al., 2015). Although many studies attempt to explain the auxiliary role of thermal stress in fracture propagation through simulations, few experiments can fully reproduce the entire process from "fluid injection-fracture propagation" to "thermal recovery after pump shutdown." This disconnects between simulation and experiment limits our in-depth understanding of complex THM coupling mechanisms, especially when involving unconventional cryogenic fluids.

In recent years, nitrogen has emerged as a promising non-aqueous working fluid, demonstrating unique advantages in geothermal and unconventional oil and gas development. Gaseous nitrogen, characterized by chemical inertness and easy flowback, is commonly used for auxiliary fracturing or as a tracer. More notably, the application of liquid nitrogen (LN_2) introduces a unique "cryogenic thermal shock" mechanism (Alqahtani et al., 2016). Unlike conventional fluids, the injection of LN_2 at -196 °C into high-temperature rock masses creates an extreme temperature gradient at the contact surface, inducing intense tensile thermal stress. This thermal stress enables thermally induced fracturing of the rock matrix at pressures below the breakdown pressure, forming a more complex network of microfractures—an innovative development for improving HDR permeability (Wang et al., 2017; Cha et al., 2014).

Despite the existing research foundation on the mechanisms of LN_2 fracturing in rocks, most literature is limited to mechanical property tests of small-scale rock samples (e.g., strength changes after uniaxial/triaxial compression) or pure theoretical simulations. Systematic experimental studies on the complete dynamic process involving rapid near-wellbore cooling, thermal stress-induced fracturing, and the influence of fracture geometry on formation thermal recovery remain insufficient. In particular, the manner in which different fracture geometries (e.g., vertical vs. horizontal fractures) inversely control thermal recovery behaviors after nitrogen injection remains unclear. Addressing this gap, this study conducted a series of large-scale true triaxial LN_2 injection and circulation experiments using concrete specimens as controllable HDR analogs. This research not only quantifies the cooling and reservoir stimulation effects of LN_2 but also for the first time explores the dominant role of fracture geometry in reservoir thermal recovery time, providing critical experimental basis for optimizing LN_2-assisted EGS development.

2 EXPERIMENTAL SETUP AND METHODOLOGY

2.1 Preparation and Characterization of Test Samples

2.1.1 Concrete Sample Preparation

Concrete blocks were used as rock analogs in this study to ensure material consistency and repeatability in cryogenic fracturing experiments. Specimens were prepared by mixing Portland cement (Type I/II) with coarse sand and water, maintaining a fixed sand-to-cement mass ratio of 2.5 and a water-to-cement ratio of 0.55. The mixture was cast into cubic molds (20 cm × 20 cm × 20 cm), cured in water for 30 days to achieve maximum strength, and then air-dried under ambient conditions for subsequent use.

To monitor the internal temperature evolution during LN_2 treatment, five T-type thermocouples (TCs) were embedded in each specimen during casting. As illustrated in Figure 1, the thermocouples were positioned at a specific depth (10 cm from the top surface) and radial distances from the wellbore to capture thermal gradients. Two thermocouples were arranged along the y-axis, and the other three along the diagonal to capture spatial temperature variations. This configuration enables precise recording of the propagation of the cooling front and the thermal recovery process within the rock matrix.

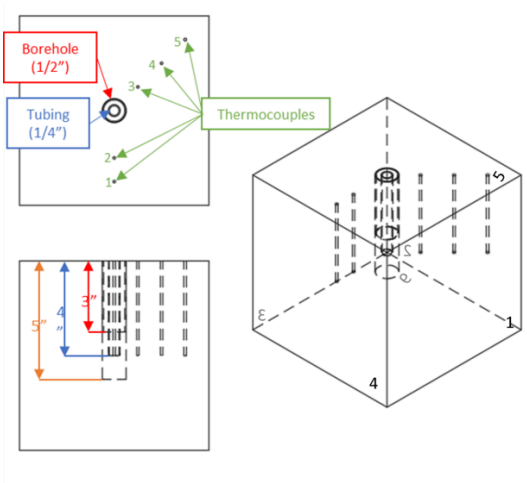


Figure 1. The schematic of a concrete sample embedded with thermocouples.

2.1.2 Material Characterization

Prior to cryogenic testing, the physical and mechanical properties of the concrete samples were characterized to provide baseline data for analysis. Key parameters including density, porosity, and permeability were measured using standard laboratory procedures. Mechanical properties such as Young's modulus, Poisson's ratio, and uniaxial compressive strength were determined through ultrasonic velocity measurements and uniaxial compression tests. These properties are summarized in Table 1 and Table 2.

Table 1. Mechanical properties of concrete samples by acoustic measurement

Property	Values
Compressional Velocity, V_p	4215 m/s
Shear Velocity, V_s	2455 m/s
Constraint Modulus, M	36.3 GPa
Shear Modulus, G	12.5 GPa
Bulk Modulus, K	20.1 GPa
Young's Modulus, E	30.0 GPa
Poisson's Ratio, υ	0.243

Table 2. Other properties of concrete samples

Property	Values
Density, ρ	2.041 g/cc
Porosity, ϕ	9.56%
Permeability, k	0.009 mD
Specific heat, c_p	891 J/(kg·K)
Tensile strength, σ_t	2.878 MPa
Uniaxial Compressional Strength, σ_c	37.343 MPa

2.2 Experimental System Configuration

To simulate the high-temperature environment of deep HDR reservoirs and achieve controlled LN_2 injection, an integrated cryogenic fracturing experimental system was established. The system primarily consists of two core subsystems: the cryogenic fluid injection system and the environmental control & monitoring system.

2.2.1 Cryogenic Fluid Injection and Transfer System

A dedicated LN_2 transfer and injection unit was designed to achieve high-pressure LN_2 injection (Figure 2 and Figure 3). The vessel, fabricated from annealed stainless steel tubing, has a capacity of approximately 0.95 L and a design pressure rating of 3.4 MPa. Equipped with multi-stage pressure regulators and vacuum-insulated pipelines, the system minimizes heat loss during transfer, ensuring that the fluid reaches the bottomhole in liquid form. Two operational modes are supported: "low-pressure circulation" uses LN2 to directly circulate through the tubing-annulus formed by the wellhead for rapid wellbore cooling, and "high-pressure injection" injects LN2 through wellbore into formation fractures.

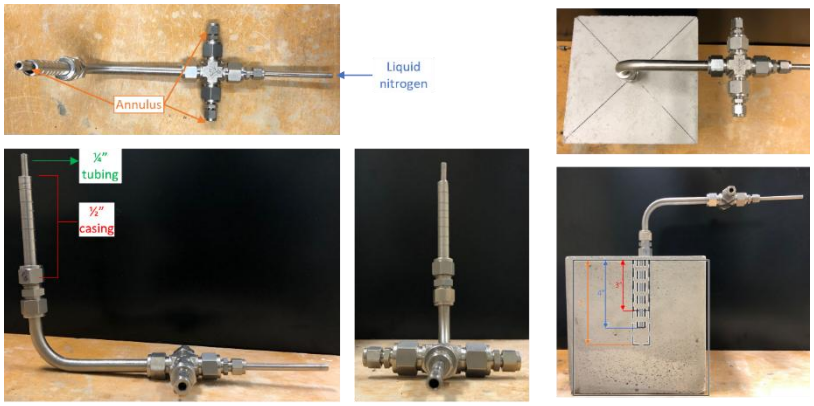


Figure 2. The schematic of a concrete sample embedded with thermocouples.

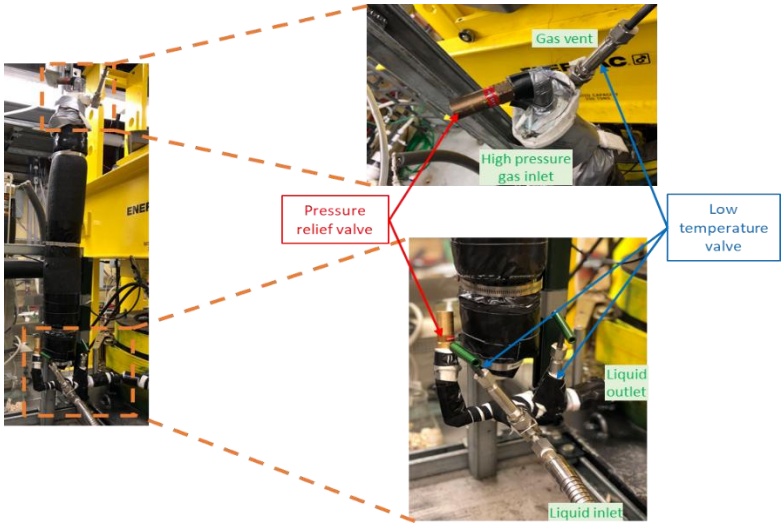


Figure 3. The LN2 transfer vessel is installed vertically and heavily insulated. There are two pressure relief valves (3.4 MPa) at the inlet (bottom) and gas vent (top) of the vessel.

2.3 Experimental Design and Procedures

To systematically evaluate the cooling efficiency and permeability enhancement effect of liquid nitrogen (LN_2) on high-temperature rocks, a standardized experimental protocol was developed, encompassing baseline permeability assessment, pre-fracturing treatment, and LN_2 injection testing under high-temperature conditions. First, the initial permeability characterization of the samples was performed via the Pressure Decay Test (PDT). Analogous to the inverse process of the well shut-in pressure buildup test in oilfield operations, this method involves injecting gas into the wellbore to a predetermined pressure, closing the valve, and recording the natural pressure decay rate to qualitatively evaluate the original permeability of the rock matrix. Subsequently, to simulate hot dry rock (HDR) reservoirs with fractures and decouple the effect of fracture geometry on heat conduction, some samples were subjected to pre-fracturing under true triaxial stress conditions. By precisely controlling the triaxial stress state (setting vertical stress to be less than or greater than horizontal stress), horizontal or vertical fractures were induced respectively, thereby constructing fracture morphology with well-defined geometric characteristics.

In the cryogenic treatment, all samples were first heated and maintained at 200 °C in a constant-temperature system to achieve thermal equilibrium. Thereafter, circulation or injection operations were conducted according to the experimental objectives: the LN_2 circulation mode was primarily used to establish a cooling baseline under pure heat conduction conditions, while the LN_2 injection mode simulated real fracturing scenarios, forcing cryogenic fluid into the formation under high pressure. During the injection process, the system real-time monitored the temperature evolution in the wellbore and the interior rock mass, and continued to record the entire warm-up period (the process of temperature recovery to ambient temperature) after the injection ceased. This warm-up time was employed as a key indicator to assess the rock's "cold storage" retention capacity. Finally, the Pressure Decay Test was performed again. By comparing the pressure decay curves before and after the treatment, the permeability enhancement effect of cryogenic thermal shock on the reservoir was intuitively quantified.

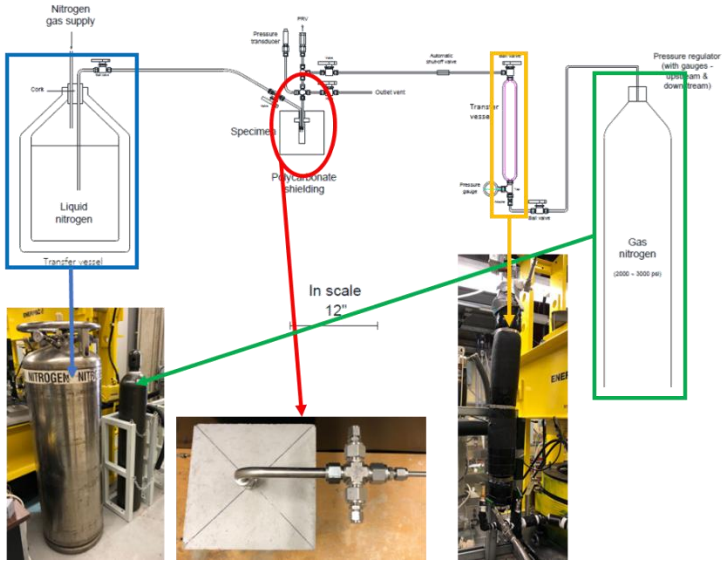


Figure 4. Experimental system schematic for cryogenic treatment on a cubic concrete block.

3 RESULTS AND ANALYSIS

This section analyses the effects of different injection pressures and pre-fracture geometries on LN_2 cryogenic fracturing and wellbore cooling efficiency. For quantitative comparison, two key evaluation indicators were selected: (1) Wellbore warm-up time: The time required for the wellbore temperature to recover to 130 °C, 140 °C, 150 °C, and 160 °C after LN_2 injection cessation, reflecting the cooling range and its "durability." (2) Pressure decay characteristics: The pressure decay curve and characteristic time for the wellbore pressure to decrease from a specific initial pressure to atmospheric pressure at 200 °C, reflecting fracture conductivity and its changes.

Based on these indicators, the coupling relationships between injection pressure, fracture geometry, and conductivity, as well as their comprehensive effects on cryogenic fracturing and cooling behavior, were analyzed for three sample types: intact samples without fractures, vertical fractured samples, and horizontal fractured samples.

3.1 Intact Samples Without Fractures

Samples C15 and C17 were intact concrete specimens without pre-fractures, where LN_2 cooling was achieved solely through heat conduction between the wellbore and the surrounding rock mass. These samples served as baselines for the "fracture-free heat conduction control" condition.

LN_2 circulation was performed at 200 °C for different durations: C15 underwent a longer circulation time with a larger injection mass, while C17's circulation time was approximately half that of C15. The test results indicate that under fracture-free conditions, the wellbore warm-up time was positively correlated with LN_2 circulation duration and total injection volume: C15 exhibited significantly longer warm-up times at all temperature recovery points compared to C17 (Table 3). This demonstrates that a longer circulation time can significantly expand the cooled volume, thereby delaying temperature recovery. These results provide a comparative baseline for analyzing complex behaviors in the presence of fractures.

Table 3. Comparison of warm-up times between Samples C15 and C17

Temp(℃) \ Sample	C15	C17
130	17.5	19.5
140	26.8	23.5
150	58.7	28.8
160	91.3	36.4

3.2 Vertical Fractured Samples

The vertical fractured group included regular blocks (C16, C18, C19, C20, C21, C22) and a "sandwich" sample (C28s), where the upper and lower layers were of conventional mix proportion, and the middle layer was a low-strength, high-permeability layer. Fractures were generated via triaxial loading and fracturing tests, roughly

vertically traversing the near-wellbore region. Compared to intact samples, vertical fractures significantly altered the flow and heat transfer paths of LN_2 in the rock mass. The experimental results are summarized in Table 4 and Table 5.

Table 4. Warm-up times to different temperature thresholds for representative samples (min)

Temp(℃) \ Sample	C16	C18	C19	C20	C22	C28s
130	17.5	98.3	62.5	10.5	48.0	22.5
140	26.8	113.0	74.9	11.1	61.5	27.9
150	58.7	129.9	89.4	11.6	77.9	35.8
160	91.3	149.8	106.9	14.9	97.8	52.7

Table 5. Key operating conditions of samples in the liquid nitrogen injection experimental group

Sample	Treatment duration	Maximum pressure	Bursting (Y/N)	Mass of LN2
C16	1200 s	20 psi	N	2.8 kg
C18	1167 s	90 psi	\	11.05 kg
C19	3200 s	83 psi	\	8.35 kg
C20	600 s	118 psi	\	8.95 kg
C22	400 s	\	Y	7.75 kg
C23	1450 s	83 psi	Y	5.85 kg
C25	1467 s	110 psi	Y	7.35 kg
C26	100 s	30 psi	N	3.95 kg
C28s	3980 s	52 psi	\	4.6 kg
C29s	2465 s	76 psi	N	5.35 kg

Sample C16 was fractured vertically at a relatively low temperature, with fractures generally vertically penetrating the near-wellbore region. At 200 °C, short-term LN_2 circulation was performed for approximately 70 s, followed by LN_2 injection at a maximum pressure of ~73 psi for 288 s, resulting in a total treatment time of 358 s and an LN_2 consumption of 7.6 kg without fracture instability. After injection cessation, the wellbore temperature recovery times to 130, 140, 150, and 160 °C were 17.5, 26.8, 58.7, and 91.3 min, respectively (Table 4). Compared to the fracture-free control samples, C16 exhibited significantly longer warm-up times in the high-temperature range (150–160 °C), indicating that vertical fractures enhanced the cooled volume in the near-wellbore region, while the overall conductivity remained at a moderate level.

The fracture morphology of Sample C18 is shown in Figure 5. C18 had the longest injection time and largest LN_2 consumption among the vertical fractured group. Pre-embedded thermocouples showed a significant temperature drop in the regions on both sides of the fracture (Figure 6), indicating a larger cooled volume. The corresponding wellbore warm-up time (Table 4) was significantly longer than that of C16, demonstrating the enhanced cooling effect achieved by the combined action of medium-high injection pressure and prolonged injection time despite the relatively small overall area of vertical fractures.

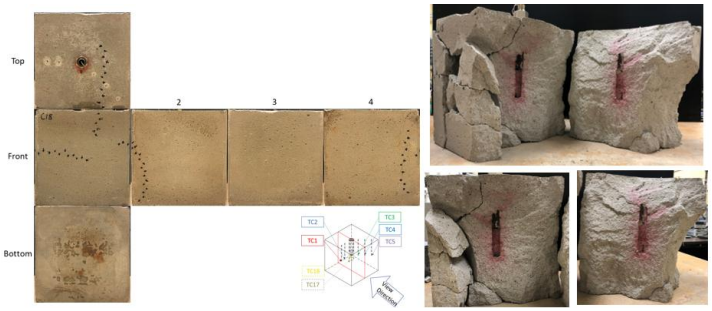


Figure 5. Pictures of C18 after LN2 injection.

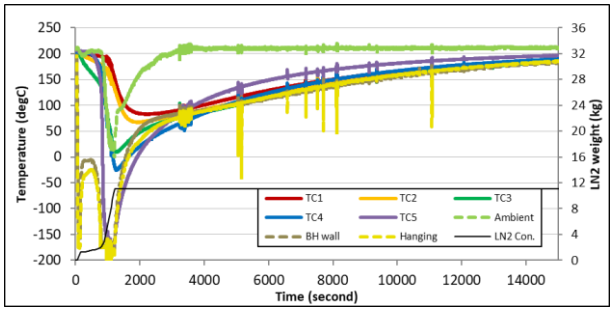


Figure 6. Temperature profile and LN2 consumption of the LN2 injection treatment on C18.

Sample C19 featured pre-formed vertical fractures penetrating the wellbore and extending upward into the sample (Figure 7). Its prolonged injection allowed sufficient time for LN_2 to infiltrate the sample interior along the vertical fractures. Pre-embedded thermocouples detected significant temperature drops both on the fracture side and in regions far from the fracture (Figure 8). The wellbore warm-up time (Table 4) was among the highest in the vertical fractured group, indicating a favorable cooled volume and durability.

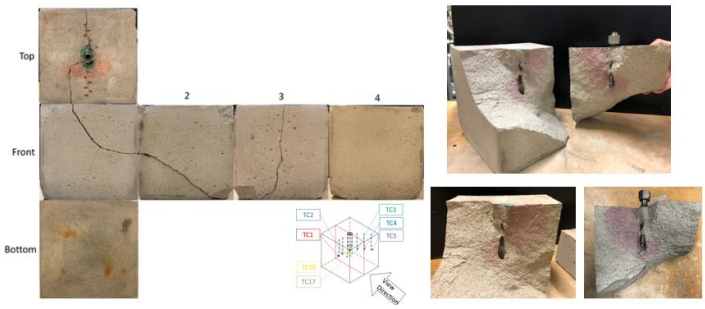


Figure 7. Pictures of C19 after LN2 injection.

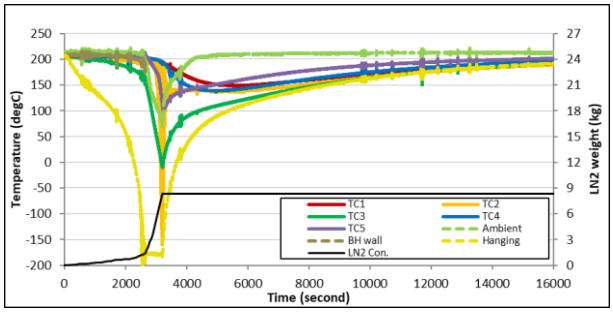


Figure 8. Temperature profile and LN2 consumption of the LN2 injection treatment on C19.

Sample C20 was subjected to short-duration, high-pressure injection with high instantaneous injection intensity. Due to the high fracture conductivity, LN_2 rapidly filled the wellbore and leaked along the fractures in the early stage of injection, resulting in localized cooling near the wellbore and a limited internal cooled volume (Figure 9). The wellbore warm-up time (Table 4) was significantly shorter than that of samples such as C18 and C19, indicating that excessively high injection pressure combined with high-conductivity fractures reduces the residence time of LN_2 within the limited-volume sample, thereby weakening the overall cooling effect.

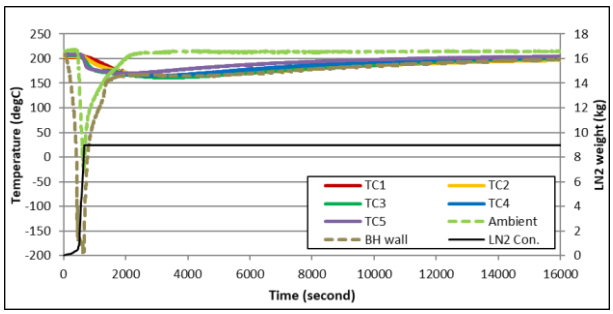


Figure 9. Temperature profile and LN2 consumption of the LN2 injection treatment on C20.

Sample C22 fractured during the high-temperature pressure decay test at 200 °C (Figure 10), exhibiting extremely high fracture conductivity, which was treated as an extreme "infinite conductivity" condition in subsequent numerical analysis. LN_2 leaked through the fractures during injection. Under this condition, localized cooling was intense, but the overall cooled volume was limited. Although the wellbore warm-up time was longer than that of intact samples, it was significantly constrained by the rapid fluid escape caused by excessively high conductivity.

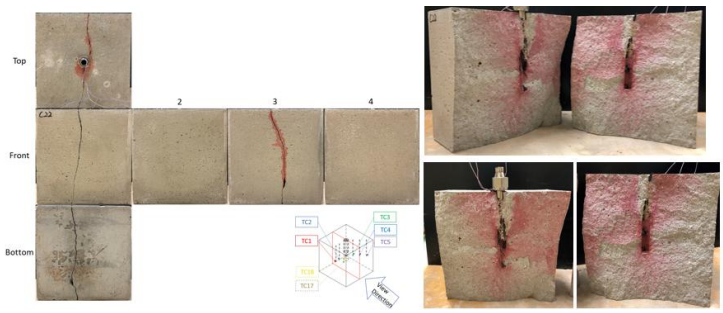


Figure 10. Pictures of C22 after LN2 injection.

Sample C28s was a "sandwich" concrete specimen. Sectional analysis revealed that vertical fractures penetrated the middle layer and extended along the x-axis at the top surface (Figure 11). The sample was subjected to medium-pressure, long-duration, low-rate injection at 200 °C with a relatively limited injection mass (Table 5). Pressure decay tests were performed at 200 °C both before and after LN_2 injection. The results showed that the initial vertical fracture conductivity was moderate, which significantly increased after LN_2 injection (Figure 12), indicating that cryogenic circulation not only enhanced cooling but also notably improved fracture conductivity.

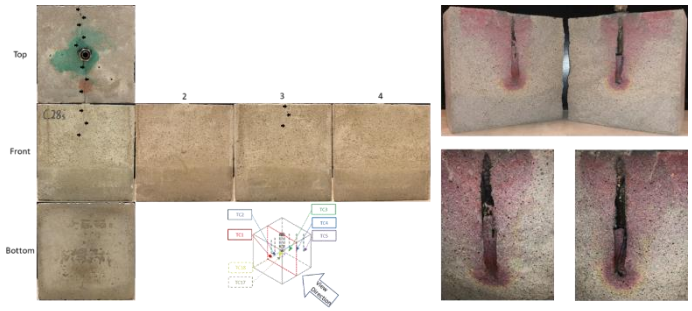


Figure 11. Pictures of C28s after LN2 injection.

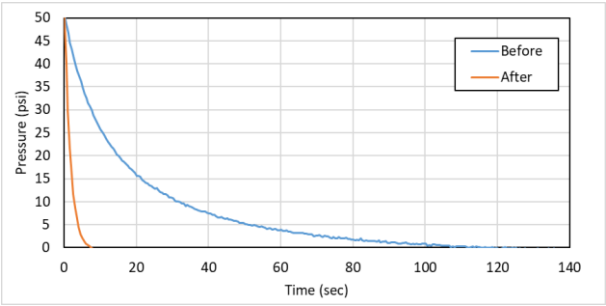


Figure 12. Pressure decay curves before and after the LN2 injection treatment on C28s.

The experimental results indicate that the wellbore warm-up time of C28s was moderate among the vertical fractured group: significantly longer than samples with short injection times or "excessive conductivity" (e.g., C16, C20), but slightly shorter than samples subjected to long-duration, medium-high pressure injection (e.g., C18, C19). Combined with the temperature curve during injection (Figure 13), pressure decay curve (Figure 12), and post-test anatomical photographs (Figure 11), it can be inferred that the interbedded structure increased the fracture surface area and heat transfer interface, resulting in a "sandwich-like low-temperature zone" in the cooled region. However, due to the limited total injection volume, the overall cooled volume was still less than that of C18 and C19.

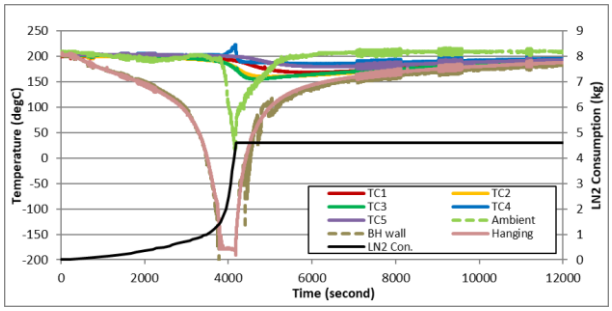


Figure 13. Temperature profile and LN2 consumption of the LN2 injection treatment on C28s.

3.3 Horizontal Fractured Samples

Samples C23, C24, C25, C26, and C29s were pre-fractured under a stress regime in which the vertical stress was the minimum principal stress; thus, horizontal fractures were expected. However, post-treatment inspection revealed the presence of inclined–horizontal fractures in several specimens. The corresponding warm-up durations for these samples are listed in Table 6.

Table 6. Warm-up times to different temperature thresholds for representative samples(min)

Temp(℃) \ Sample	C23	C24	C25	C26	C29s
130	15.4	7.4	96.1	36.6	98.8
140	20.5	8.5	107.8	45.8	115.9
150	29.2	11.2	124.4	56.2	138.0
160	44.1	18.3	144.2	71.0	159.7

Sample C23 was injected at medium-high pressure for a moderate duration. Due to thermal damage to the thermocouple connectors, some temperature data were abnormal. The warm-up time of C23 was only qualitatively determined to be significantly longer than that of intact samples, indicating that horizontal fractures can form larger cooled volumes under medium-high pressure injection.

Sample C24 was subjected to short-duration, high-pressure injection. The wellbore pressure increased significantly in the late stage of injection, inducing fracture re-opening. Its wellbore warm-up time was extremely short, indicating that although the fracture conductivity was high and localized cooling was intense, the residence time of LN_2 within the sample was limited, resulting in a small overall cooled volume.

Sample C25 underwent long-duration, high-pressure injection. As the injection progressed, the fractures gradually fully opened, leading to a significant increase in flow rate and eventual sample fracture (Figure 14). The wellbore temperature recovery times to 130 and 140 °C were approximately 96.1 and 107.8 min, respectively, significantly longer than those of C24. This indicates that under conditions of high conductivity and prolonged injection, horizontal fractures can form extremely deep, large-volume cooled regions.

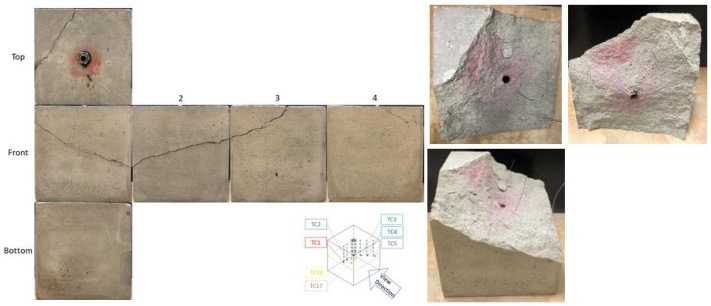


Figure 14. Pictures of C25 after LN2 injection.

Sample C26 was injected at medium pressure for a short duration. Sectional analysis revealed a major horizontal fracture and a vertical fracture, forming a complex fracture network (Figure 15). Despite the short LN_2 injection time, the complex fractures provided favorable flow paths, resulting in considerable overall cooling efficiency.



Figure 15. Pictures of C26 after LN2 injection.

Sample C29s was a horizontal fractured "sandwich" specimen, incorporating an internal interlayer on the basis of pre-formed fractures, resulting in a more complex fracture surface. The test was conducted at 200 °C with medium-high pressure, long-duration injection, and the sample fractured at the end of the test.

The wellbore warm-up time of C29s was among the longest among all concrete samples, with warm-up times at multiple temperature points comparable to or even longer than those of samples such as C25 and C18 (Table 6). Thermal imaging and sectioning results (Figure 16 and Figure 17) showed the formation of a distinct low-temperature extension zone around the wellbore. The cooling influence extended not only along the main fracture direction but also formed multi-layered cooling zones within the interlayer region.

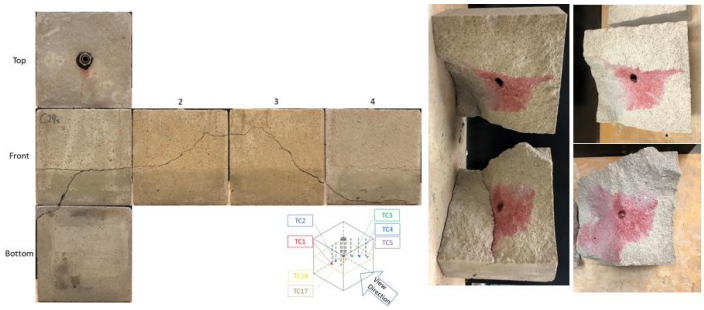


Figure 16. Pictures of C29 after LN2 injection.

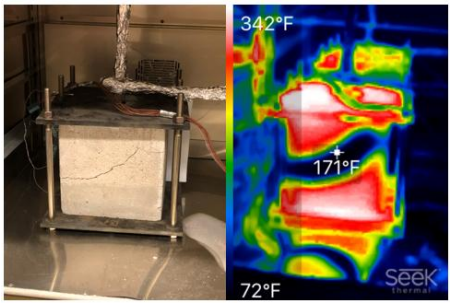


Figure 17. Thermal image of C29s during LN2 injection.

3.4 Comparison and Summary

3.4.1 Effect of Injection Pressure

In the vertical fractured group, Samples C18 (90 psi, 1167 s injection) and C19 (83 psi, 3200 s injection) were subjected to medium-high pressure and prolonged injection, resulting in significantly longer wellbore warm-up times compared to C16 (73 psi, 358 s injection) and C20 (118 psi, 600 s injection).

In the vertical fractured group, the warm-up time of C20 was significantly shorter than that of samples such as C18 and C19, indicating that within a certain range, higher injection pressure is often associated with greater fracture conductivity and shorter LN_2 residence time, thereby reducing warm-up time.

In the horizontal fractured group, Sample C24 exhibited the highest peak pressure (~148 psi) but short injection time and extremely short warm-up time; in contrast, Samples C25 and C29s were injected continuously at high pressure, leading to complete fracture re-opening or even fracture, resulting in significantly increased cooled volume and warm-up time.

Overall, injection pressure alone is not the sole determinant of cooling efficiency: insufficient pressure fails to initiate or re-open fractures, limiting the cooling range; excessively high pressure combined with extremely high conductivity causes rapid LN_2 leakage, reducing effective cooling time. A comprehensive consideration of fracture conductivity and injection duration is required.

3.4.2 Effect of Fracture Orientation and Morphology

Fracture orientation is one of the most important factors influencing wellbore warm-up time: under similar conditions, horizontal (or near-horizontal) fractures are more effective to extending warm-up time, with cooled volumes typically larger than those of vertical fractures.

Fracture morphology and internal fracture area are equally critical: samples with inclined horizontal or composite fractures (e.g., C25, C26, C29s) feature larger internal fracture surface coverage. Pre-embedded thermocouples showed that the cooling zone extended more widely across the sample cross-section, corresponding to longer warm-up times.

Therefore, under the same injection pressure and conductivity level, horizontal/inclined horizontal fractures are more effective to vertical fractures for forming large-volume low-temperature zones.

3.4.3 Fracture Conductivity and Pressure Decay Results

The pressure decay curve of C28s before LN_2 injection indicated moderate vertical fracture conductivity; after injection, pressure decay accelerated significantly, and conductivity increased to a high level. This demonstrates that LN_2 cryogenic treatment not only cools the rock mass but also significantly improves fracture conductivity.

For samples with "extremely high" conductivity (e.g., C22, C25), pressure decay was very rapid. During injection, LN_2 could quickly re-open fractures and escape. Although localized cooling was intense, the effective cooled volume and warm-up time were limited.

In summary, once fracture conductivity is sufficient to ensure smooth injection, moderately low conductivity is more favorable for extending the residence time and heat transfer contact time of LN_2 in the rock mass, thereby achieving longer warm-up times; excessively high conductivity leads to rapid "short-circuit" escape of LN_2, reducing cooling efficiency.

4 CONCLUSIONS

In this study, high-temperature (200 °C) concrete specimens were used as HDR analogs to conduct LN_2 circulation and injection experiments under true triaxial stress conditions. The cooling efficiency and reservoir stimulation effect of cryogenic thermal shock in the near-wellbore zone were systematically evaluated. Based on the comprehensive analysis of multi-point temperature monitoring and pressure decay testing, the main conclusions are as follows:

(1) Wellbore warm-up time serves as a critical indicator for comprehensively evaluating cooling efficiency. This indicator effectively integrates rock thermal diffusivity, fracture geometry, and fluid-rock heat transfer efficiency, verifying the feasibility of the rock mass acting as a "cold battery" after LN_2 injection.
(2) Under the same temperature and injection conditions, horizontal/inclined horizontal fractures are more conducive to extending warm-up time compared to vertical fractures. This geometric structure not only increases the heat transfer area but also effectively blocks vertical heat flow replenishment from the formation. In contrast to the rapid fluid escape prone to vertical fractures, horizontal fractures significantly extend warm-up time.
(3) An "optimal range" exists between injection pressure and fracture conductivity. The optimal cooling effect is achieved under moderate conductivity and appropriate injection pressure, where LN_2 can be smoothly injected while maintaining sufficient heat transfer time to cool the deep rock matrix.
(4) LN_2 cryogenic circulation/injection can significantly alter fracture conductivity. This indicates that LN_2 is not only a cooling medium but also an efficient waterless stimulation tool, particularly suitable for improving the initial permeability of high-temperature tight formations.

In conclusion, to maximize the heat extraction potential of LN_2 in field EGS development, engineering design should not solely pursue large single fracture width but rather focus on constructing a fracture system dominated by horizontal or complex network fractures with moderate conductivity. This approach can leverage the formation of cooling zones to extend low-temperature retention time while avoiding rapid ineffective loss of working fluid, thereby enhancing the economic efficiency of geothermal exploitation.

Acknowledgements

The authors would like to acknowledge the Natural Science Foundation of China (52304058, 5233000503, U24B6001), the Oil & Gas Major Project 'New-Generation Key Technologies and Equipment for Complex Reservoir Stimulation' (2024ZD1404701), and the Science Foundation of China University of Petroleum, Beijing (No. 2462023BJRC013) for funding this research.

REFERENCES <HEADING STYLE>

BP plc.: BP 2017 Statistical Review of World Energy, Proceedings, Energy Statistics Workshop, London, United Kingdom (2018).

Global CCS Institute.: The Global Status of CCS 2013, Proceedings, Carbon Capture & Storage Workshop, Canberra, Australia (2013).

Matek, B.: 2016 Annual U.S. & Global Geothermal Power Production Report, Proceedings, Geothermal Development Workshop, Washington, D.C., United States (2016).

Brown, D.W.: A hot dry rock geothermal energy concept utilizing supercritical CO_2 instead of water, Proceedings, Twenty-Fifth Workshop on Geothermal Reservoir Engineering, Stanford University, Stanford, USA (2000), 233–238.

Pruess, K.: Enhanced geothermal systems (EGS) using CO_2 as working fluid – a novel approach for generating renewable energy with simultaneous sequestration of carbon, Geothermics, 35, (2006), 351–367.

Xu, R.N., Zhang, L., Zhang, F.Z., and Jiang, P.X.: A review on heat transfer and energy conversion in the enhanced geothermal systems with water/CO_2 as working fluid, International Journal of Energy Research, 39, (2015), 1722–1741.

Harto, C., Schroeder, J., Horner, R., and Clark, C.: Geothermal energy and the energy–water nexus, Proceedings, Thirty-Eighth Workshop on Geothermal Reservoir Engineering, Stanford University, Stanford, USA (2013).

Xu, T.F., Pruess, K., and Apps, J.: Numerical studies of fluid–rock interactions in enhanced geothermal systems (EGS) with CO_2 as working fluid, Proceedings, Thirty-Third Workshop on Geothermal Reservoir Engineering, Stanford University, Stanford, USA (2008).

Fouillac, C., Sanjuan, B., Gentier, S., and Czernichowski-Lauriol, I.: Could sequestration of CO_2 be combined with the development of enhanced geothermal systems?, Proceedings, Third Annual Conference on Carbon Capture and Sequestration, Alexandria, USA (2004).

Global CCS Institute: Introduction to carbon capture and storage, Global Status of CCS 2016: Special Report, Global CCS Institute (2016).

Buscheck, T.A., Bielicki, J.M., Randolph, J.B., Chen, M., Hao, Y., Edmunds, T.A., Adams, B., and Sun, Y.: Multi-fluid geothermal energy systems in stratigraphic reservoirs: Using brine, N_2, and CO_2 for dispatchable renewable power generation and bulk energy storage, Proceedings, Thirty-Ninth Workshop on Geothermal Reservoir Engineering, Stanford University, Stanford, USA (2014).

Buscheck, T.A., Bielicki, J.M., Chen, M., Sun, Y., Hao, Y., Edmunds, T.A., Randolph, J.B., and Saar, M.O.: Multi-fluid sedimentary geothermal energy systems for dispatchable renewable electricity, Proceedings, World

Alqahtani, N.B., Cha, M., Yao, B., Yin, X., Kneafsey, T.J., Wang, L., Wu, Y.-S., and Miskimins, J.L.: Experimental investigation of cryogenic fracturing of rock specimens under true triaxial confining stresses, Proceedings, SPE Europec featured at 78th EAGE Conference and Exhibition, Vienna, Austria (2016).

Wang, L., Yao, B., Cha, M., Alqahtani, N.B., Wu, Y.-S., Kneafsey, T., Miskimins, J., Yin, X., and Patterson, T.: Waterless fracturing technologies for unconventional reservoirs – opportunities for liquid nitrogen, Journal of Natural Gas Science and Engineering, 35, (2016), 160–174.

Cha, M., Yin, X., Kneafsey, T., Johanson, B., Alqahtani, N., Miskimins, J., Patterson, T., and Wu, Y.-S.: Cryogenic fracturing for reservoir stimulation—laboratory studies, Journal of Petroleum Science and Engineering, 124, (2014), 436–450.